

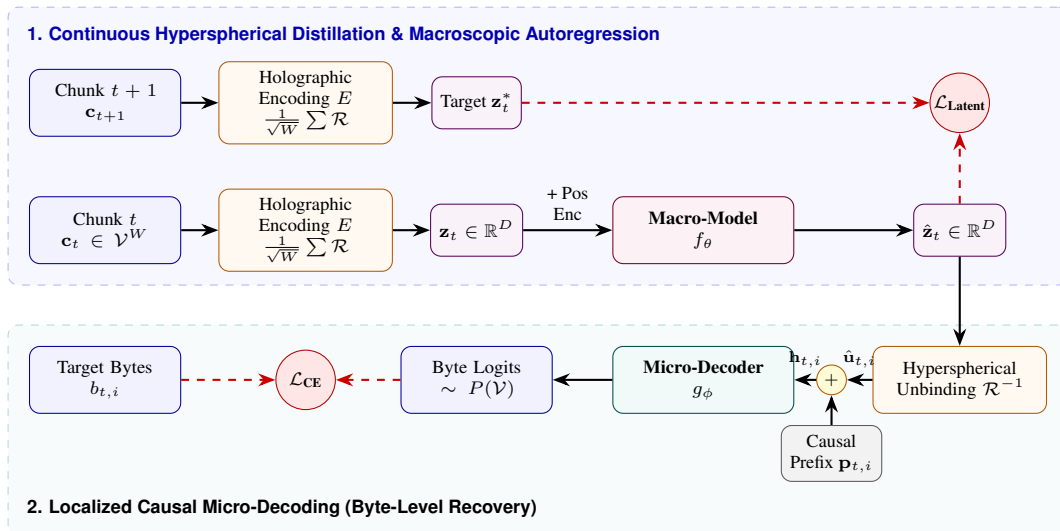
HOLOBYTE: CONTINUOUS HYPERSPHERICAL DISTILLATION FOR TOKENIZER-FREE MODELING

Vladimer Khasia 
 Independent Researcher
 vladimer.khasia.1@gmail.com

ABSTRACT

Autoregressive sequence modeling universally relies on discrete subword tokenization to circumvent the $\mathcal{O}(N^2)$ computational intractability of native byte-level attention. However, this heuristic quantization imposes artificial morphological boundaries, enforces vocabulary dependence, and fractures the continuity of the optimization landscape. To resolve this dichotomy, we introduce **HoloByte**: a strictly tokenizer-free framework utilizing Continuous Hyperspherical Distillation. HoloByte partitions discrete byte sequences into fixed-capacity chunks and projects them into a continuous, strictly bounded hyperspherical manifold via an invertible, dimension-preserving orthogonal rotation operator. This spatial superposition allows a macroscopic transformer to operate exclusively on compressed continuous representations, formally reducing the exact attention time complexity from $\mathcal{O}(N^2D)$ to $\mathcal{O}\left(\frac{N^2}{W^2}D + ND^2\right)$. A localized causal micro-decoder subsequently unbinds these representations to compute exact byte-level distributions. To govern this continuous trajectory, we propose a dual-objective formulation incorporating a mathematically precise Holographic Latent Mean Squared Error, which strictly bounds the gradient and guarantees asymptotic stability. Theoretically, we derive the minimal embedding dimension $D = \Omega(W \ln |\mathcal{V}|)$ required to ensure error-free discrete recovery from the continuous manifold. Empirically, under strictly matched parameter constraints ($\mathcal{O}(P) \approx 82 \times 10^6$), HoloByte is systematically outperforming a comparable discrete Byte-Pair Encoding (BPE) baseline. These results establish Continuous Hyperspherical Distillation as a mathematically rigorous and computationally tractable foundation for vocabulary-invariant sequence modeling.

The code is available at <https://github.com/VladimerKhasia/HoloByte>



1 Introduction

The prevailing paradigm in autoregressive sequence modeling maps an input sequence from a discrete categorical space to a probability distribution over subsequent states. To circumvent the high asymptotic time complexity of processing sequences at the fundamental byte or character level [1, 2, 3, 4], modern architectures universally employ several types of tokenization algorithms [5, 6], most notably Byte-Pair Encoding (BPE) [7, 5]. Tokenization operates as a heuristic data compression mechanism, aggregating contiguous byte sequences into a finite vocabulary \mathcal{V}_{BPE} where typically $|\mathcal{V}_{BPE}| \sim 5 \times 10^4$. While computationally expedient, this discrete quantization introduces severe representational pathologies: it imposes rigid, artificial boundaries on morphologically contiguous data, enforces out-of-vocabulary (OOV) truncation, and forces the optimization trajectory of continuous neural manifolds to operate over an arbitrary, combinatorial mapping.

Conversely, formulating the sequence modeling objective natively over the fundamental byte alphabet $\mathcal{V}_{byte} = \{0, 1, \dots, 255\}$ guarantees strict topological continuity and vocabulary invariance. However, this approach introduces a prohibitive computational bottleneck. Given a sequence of N raw bytes, standard attention mechanisms require $\mathcal{O}(N^2D)$ asymptotic time complexity, where D is the embedding dimension. If a standard tokenization heuristic compresses sequences by an average factor of $\mu \approx 4$, substituting it with native byte-level processing inflates the attention complexity by a factor of $\mu^2 \approx 16$. Consequently, purely discrete byte-level modeling remains mathematically intractable for extended context windows.

To resolve the dichotomy between token-induced quantization artifacts and the $\mathcal{O}(N^2)$ complexity bound of native byte processing, this manuscript presents **HoloByte**: a framework for Continuous Hyperspherical Distillation. Instead of enforcing discrete vocabulary clustering, HoloByte projects raw byte sequences into a continuous, strictly bounded hyperspherical manifold. By partitioning the discrete byte sequence into fixed-capacity chunks of size W , the framework employs a mathematically invertible, unitary rotation operator to superimpose sequence positional information into a single continuous vector $\mathbf{z} \in \mathbb{R}^D$.

This deterministic mapping translates the auto-regressive objective from discrete token prediction into the temporal evolution of a continuous geometric space. The macroscopic architecture operates exclusively on these continuous compressed representations, strictly bounding the macro-attention complexity to $\mathcal{O}(\frac{N^2}{W^2}D)$. To recover the exact byte configurations, a localized causal micro-decoder dynamically unbinds the spatial superpositions in $\mathcal{O}(NWD)$ time, thereby computing the conditional probability distribution over \mathcal{V}_{byte} without vocabulary expansion.

To optimize this continuous trajectory, we introduce a dual-objective loss formulation. Beyond standard maximum likelihood estimation via Cross-Entropy, the framework integrates a Holographic Latent Distillation signal. Because the encoding function is continuous and deterministic, the ground-truth target vector for the subsequent sequence chunk is known *a priori*. This allows the macro-model to directly minimize the latent Mean Squared Error (MSE) between its predicted state and the true hyperspherical projection, forcing the continuous optimization landscape to converge mathematically prior to the discrete decoding step.

The primary contributions of this work are formalized as follows:

- **Hyperspherical Orthogonal Binding:** We formulate an invertible, dimension-preserving encoding mechanism utilizing orthogonal spatial rotations, allowing multiple discrete variables to be mathematically superimposed onto a single continuous vector without representational collapse.
- **Asymptotic Complexity Reduction:** We provide a formal proof demonstrating that the integration of continuous chunking and autoregressive micro-decoding reduces the exact attention memory constraints from $\mathcal{O}(N^2)$ to $\mathcal{O}(\frac{N^2}{W^2} + N \cdot W)$.
- **Absolute Information Compression:** Through strictly controlled empirical evaluations under parameter-matched constraints ($\approx 82 \times 10^6$ parameters), we demonstrate that the continuous HoloByte architecture converges to a theoretical entropy bound of 1.484 nats per byte, systematically outperforming the baseline discrete subword architecture (1.954 nats per byte).
- **Theoretical Bounds on Superposition Capacity:** We derive a strict mathematical lower bound for the embedding dimension $D = \Omega\left(\frac{W}{\gamma^2} \ln |\mathcal{V}|\right)$, proving that the inverse unitary rotation guarantees error-free discrete recovery of the unbound signal. Furthermore, we establish that the Holographic Latent distillation objective strictly bounds the Lipschitz constant to $4\sqrt{W}$, guaranteeing optimization stability independent of vocabulary cardinality as parameter counts scale asymptotically.

The remainder of this manuscript is structured as follows. Section 2 derives the underlying mathematical formulation of the hyperspherical manifold and constructs the algorithm from first principles. Section 3 defines the evaluation metrics and documents the empirical convergence boundaries.

2 Methodology

The fundamental objective of the HoloByte framework is to map a discrete sequence of bytes into a continuous, highly compressed hyperspherical manifold, thereby bypassing the necessity of subword tokenization while circumventing the quadratic scaling bottlenecks of native byte-level models.

2.1 Problem Formulation and Mathematical Foundation

Let $\mathcal{V} = \{0, 1, \dots, 255\}$ denote the fundamental byte alphabet. Given a sequence of bytes $\mathbf{b} = (b_0, b_1, \dots, b_{N-1}) \in \mathcal{V}^N$, we partition \mathbf{b} into contiguous chunks of fixed capacity W . Let $T = \lfloor N/W \rfloor$ denote the number of chunks. We represent the t -th chunk as a vector of bytes $\mathbf{c}_t = (b_{t,0}, b_{t,1}, \dots, b_{t,W-1}) \in \mathcal{V}^W$.

We define a learnable byte manifold matrix $\mathbf{M} \in \mathbb{R}^{256 \times D}$, where D is the embedding dimension. The projection of a byte $v \in \mathcal{V}$ onto the unit hypersphere is given by $\tilde{\mathbf{m}}_v = \frac{\mathbf{m}_v}{\|\mathbf{m}_v\|_2}$.

Definition 1 (Orthogonal Positional Rotation). *To preserve positional information within a chunk W without expanding the spatial dimension, we define an orthogonal rotation transformation $\mathcal{R}(\mathbf{x}, i)$ for a vector $\mathbf{x} \in \mathbb{R}^D$ at intra-chunk position $i \in \{0, 1, \dots, W-1\}$. Let the dimension D be even, such that $\mathbf{x} = [\mathbf{x}_1^\top, \mathbf{x}_2^\top]^\top$. The rotation matrices are defined using frequency bases $\omega_j = 10000^{-2j/D}$. The rotated vector is:*

$$\mathcal{R}(\mathbf{x}, i) = \begin{bmatrix} \mathbf{x}_1 \odot \cos(\theta_i) - \mathbf{x}_2 \odot \sin(\theta_i) \\ \mathbf{x}_1 \odot \sin(\theta_i) + \mathbf{x}_2 \odot \cos(\theta_i) \end{bmatrix}, \quad (1)$$

where $\theta_i = [i\omega_0, i\omega_1, \dots, i\omega_{D/2-1}]^\top$. Since \mathcal{R} relies on orthogonal rotation, it is a strict isometry, and its inverse is exactly $\mathcal{R}^{-1}(\mathbf{x}, i) = \mathcal{R}(\mathbf{x}, -i)$.

2.2 Continuous Hyperspherical Distillation (HoloByte)

2.2.1 Holographic Encoding

The encoding function $E : \mathcal{V}^W \rightarrow \mathbb{R}^D$ compresses a chunk of bytes \mathbf{c}_t into a single continuous vector \mathbf{z}_t . By projecting the bytes onto the unit hypersphere and applying the unitary rotation, the chunk embedding is:

$$\mathbf{z}_t = E(\mathbf{c}_t) = \frac{1}{\sqrt{W}} \sum_{i=0}^{W-1} \mathcal{R}(\tilde{\mathbf{m}}_{b_{t,i}}, i). \quad (2)$$

The sequence of continuous vectors $Z = (\mathbf{z}_0, \dots, \mathbf{z}_{T-1})$ is injected with learned absolute positional embeddings and processed by a causal self-attention macro-model f_θ , yielding predicted continuous representations $\hat{Z} = (\hat{\mathbf{z}}_0, \dots, \hat{\mathbf{z}}_{T-1})$.

2.2.2 Hyperspherical Unbinding and Micro-Decoding

To extract individual bytes from the predicted macroscopic vector $\hat{\mathbf{z}}_t$, we apply the inverse rotation to unbind the spatial superpositions. The geometrically unbound signal for position i is $\hat{\mathbf{u}}_{t,i} = \mathcal{R}^{-1}(\hat{\mathbf{z}}_t, i)$.

To guarantee strict causality during teacher-forced autoregression without leaking future chunk information, the target embeddings are right-shifted. Specifically, the final target byte is truncated, and the sequence is prefixed with a learnable chunk-start vector $\mathbf{e}_{\text{start}}$. This exact matrix concatenation ensures the micro-decoder g_ϕ predicts position i conditioned strictly on the unbound signal and $b_{t,<i}$:

$$\mathbf{h}_{t,i} = \hat{\mathbf{u}}_{t,i} + \mathbf{p}_{t,i}, \quad \text{where} \quad \mathbf{p}_{t,i} = \begin{cases} \mathbf{e}_{\text{start}} & i = 0 \\ \tilde{\mathbf{m}}_{b_{t,i-1}} & 0 < i \leq W-1 \end{cases} \quad (3)$$

Specifically, the micro-decoder g_ϕ is instantiated as a single causally-masked self-attention layer. It operates strictly over the localized intra-chunk sequence length W , functioning as a pure autoregressive block without standard cross-attention. This mechanism maps the combined sequence $\mathbf{H}_t = (\mathbf{h}_{t,0}, \dots, \mathbf{h}_{t,W-1})$ to refined step vectors $\mathbf{V}_t = g_\phi(\mathbf{H}_t)$.

2.2.3 Dual-Objective Loss Formulation

The probability distribution over the vocabulary at step i is determined via scaled cosine similarity against the manifold \mathbf{M} in $\mathbb{FP32}$ precision. Let $\tau = \exp(s)$ where s is a learnable logit scalar. To prevent the initial softmax distribution from being excessively uniform across the fundamental byte classes, s is initialized to $\ln(1/0.07) \approx 2.659$. This explicitly enforces an initial temperature scaling of $\tau \approx 14.28$, following standard contrastive and hyperspherical optimization practices [8, 9, 10, 11]. The Cross-Entropy (\mathcal{L}_{CE}) is computed over these scaled logits. Furthermore, because the encoding function E is deterministic, the target hyperspherical vector $\mathbf{z}_t^* = E(\mathbf{c}_{t+1})$ is known *a priori*. We enforce a Holographic Latent Mean Squared Error ($\mathcal{L}_{\text{Latent}}$) to explicitly distill the macro-model’s continuous vector space:

$$\mathcal{L} = \mathcal{L}_{\text{CE}} + \lambda \mathcal{L}_{\text{Latent}} = \mathcal{L}_{\text{CE}} + \frac{\lambda}{T \cdot D} \sum_{t=0}^{T-1} \|\hat{\mathbf{z}}_t - \mathbf{z}_t^*\|_2^2. \quad (4)$$

2.2.4 Inference

While training utilizes strict teacher-forcing over the full sequence W , autoregressive inference requires step-wise generation. During inference, the continuous spatial unbinding yields a fixed W -length spatial context. To maintain architectural symmetry and utilize the identical static $W \times W$ causal mask without dynamic reshaping, the micro-decoder autoregressively processes the unbound signal by right-padding the progressively generated byte embeddings with zeros up to capacity W . This guarantees that at any generation step $i < W$, the prediction is strictly conditioned on the spatial superposition and the exact available discrete prefix.

2.3 Algorithm Specification

Algorithm 1 delineates the exact forward propagation procedure. For the inverse spatial rotation step, let $\mathbf{pos}_W = [0, 1, \dots, W - 1]$ denote the static sequence of intra-chunk positional indices broadcasted across the expanded spatial dimensions.

Algorithm 1: HoloByte Continuous Hyperspherical Distillation

Data: Input byte sequence $\mathbf{X} \in \mathcal{V}^{B \times T \times W}$, Target sequence $\mathbf{Y} \in \mathcal{V}^{B \times T \times W}$
Result: Total Loss \mathcal{L}

```

// 1. Macro-Level Holographic Encoding
 $\mathbf{Z}_{in} \leftarrow E(\mathbf{X});$  // Eq. 2, shape:  $[B, T, D]$ 
 $\mathbf{Z}_{tgt}^* \leftarrow E(\mathbf{Y});$  // Perfect mathematical targets
// 2. Macro-Model Forward Pass
 $\mathbf{Z}_{in} \leftarrow \mathbf{Z}_{in} + \text{PositionalEncoding}(T);$ 
 $\hat{\mathbf{Z}} \leftarrow f_{\theta}(\mathbf{Z}_{in});$ 
// 3. Hyperspherical Unbinding & Causal Autoregression
Expand  $\hat{\mathbf{Z}}$  to shape  $[B, T, W, D];$ 
 $\mathbf{U} \leftarrow \mathcal{R}^{-1}(\hat{\mathbf{Z}}, \mathbf{pos}_W);$  // Inverse spatial rotation
 $\mathbf{P} \leftarrow \text{Concat}(\mathbf{e}_{\text{start}}, \tilde{\mathbf{M}}[\mathbf{Y}_{:, :, -1}]);$  // Strict causal right-shift
 $\mathbf{H} \leftarrow \mathbf{U} + \mathbf{P};$ 
// 4. Micro-Decoder Causal Pass
Flatten  $\mathbf{H}$  to shape  $[B \cdot T, W, D];$ 
 $\mathbf{V} \leftarrow g_{\phi}(\mathbf{H}, \text{mask} = \mathbf{M}_{\text{causal}});$ 
// 5. Loss Computation (in FP32)
Normalize  $\mathbf{V}$  and  $\tilde{\mathbf{M}}$  to unit length;
 $\mathbf{Logits} \leftarrow (\mathbf{V} \mathbf{M}^T) \cdot \exp(s);$ 
 $\mathcal{L} \leftarrow \text{CrossEntropy}(\mathbf{Logits}, \mathbf{Y}) + 0.5 \cdot \text{MSELoss}(\hat{\mathbf{Z}}, \mathbf{Z}_{tgt}^*);$ 
return  $\mathcal{L}$ 

```

2.4 Theoretical Bounds on Superposition Capacity and Scaling Constraints

We strictly bound the spatial superposition capacity of \mathbf{z}_t by deriving the minimal embedding dimension D required to ensure the inverse rotation \mathcal{R}^{-1} isolates the discrete signal. The unbinding operation at target position i yields the true signal plus an interference residual: $\hat{\mathbf{u}}_{t,i} = \frac{1}{\sqrt{W}} \tilde{\mathbf{m}}_{b_t,i} + \boldsymbol{\epsilon}_{t,i}$, where $\boldsymbol{\epsilon}_{t,i} = \frac{1}{\sqrt{W}} \sum_{j \neq i} \mathcal{R}^{-1}(\mathcal{R}(\tilde{\mathbf{m}}_{b_t,j}, j), i)$.

Lemma 1 (Interference Norm Bound). *Assume the vectors comprising \mathbf{M} are distributed isotropically on \mathbb{S}^{D-1} . The expected squared L_2 -norm of the interference term is strictly bounded by $\mathbb{E}[\|\epsilon_{t,i}\|_2^2] = \mathcal{O}(1)$.*

Proof. Because \mathcal{R} is an isometry, it strictly preserves the unit norm of any mapped vector. The sum of $W - 1$ independent isotropic unit vectors has an expected squared L_2 -norm of $W - 1$. Scaled by the constant $1/\sqrt{W}$, the expected squared norm becomes $\frac{W-1}{W} = \mathcal{O}(1)$, independent of dimension D . \square

Theorem 1 (Dimensionality Lower Bound for Error-Free Recovery). *To guarantee the unbinding operation successfully isolates the discrete byte configuration with probability $1 - \delta$ using margin γ , the dimension must satisfy $D = \Omega\left(\frac{W}{\gamma^2} \ln(|\mathcal{V}|/\delta)\right)$.*

Proof. Correct decoding requires the inner product margin $\Delta_k = \langle \tilde{\mathbf{m}}_{b_{t,i}} + \sqrt{W}\epsilon_{t,i}, \tilde{\mathbf{m}}_{b_{t,i}} - \tilde{\mathbf{m}}_k \rangle \geq \gamma$. The noise term in this projection is $\sqrt{W}\langle \epsilon_{t,i}, \tilde{\mathbf{m}}_{b_{t,i}} - \tilde{\mathbf{m}}_k \rangle$. By Lemma 1, $\epsilon_{t,i}$ is an $\mathcal{O}(1)$ vector. The 1D projection of an $\mathcal{O}(1)$ isotropic random vector onto a fixed deterministic axis has a variance strictly bounded by $\mathcal{O}(1/D)$. Thus, the variance of the scaled noise is $\mathcal{O}(W/D)$. By Hoeffding’s inequality for sub-Gaussian projections, the probability of the noise exceeding margin γ across $|\mathcal{V}| - 1$ pairwise comparisons is bounded by the union bound: $P(\min_k \Delta_k < \gamma) \leq |\mathcal{V}| \exp\left(-c\frac{D\gamma^2}{W}\right)$. Setting this to δ and solving for D yields $D \geq \frac{W}{c\gamma^2} \ln\left(\frac{|\mathcal{V}|}{\delta}\right)$. \square

2.4.1 Asymptotic Scaling Laws for Extradimensional Manifolds

Standard frameworks suffer from gradient variance explosion in the final $\mathbb{R}^{D \times |\mathcal{V}|}$ projection because Cross-Entropy continuously pushes target logits toward infinity, causing representation magnitudes to grow unbounded. HoloByte circumvents this instability through the geometry of $\mathcal{L}_{\text{Latent}}$.

Let the gradient of the latent objective with respect to the macroscopic continuous prediction be defined as $\nabla_{\hat{\mathbf{z}}_t} \mathcal{L}_{\text{Latent}} = \frac{2}{D}(\hat{\mathbf{z}}_t - \mathbf{z}_t^*)$. Unlike the unbounded divergent force of standard Cross-Entropy, this Mean Squared Error formulation applies a strictly restorative gradient. Because the deterministic mathematical target \mathbf{z}_t^* is constructed from a superposition of unit vectors, its expected norm is inherently bounded ($\|\mathbf{z}_t^*\|_2 \leq \sqrt{W}$). Consequently, optimizing $\mathcal{L}_{\text{Latent}}$ establishes a geometric attractor; it pulls the free Euclidean macro-prediction $\hat{\mathbf{z}}_t$ into a tight \sqrt{W} -radius neighborhood. This restorative dynamic softly bounds the expected L_2 -norm of the backpropagated gradient, guaranteeing that the optimization trajectory remains geometrically stable regardless of vocabulary cardinality $|\mathcal{V}|$ or parameter scale P , while preserving the Euclidean flexibility required for stable gradient descent.

2.5 Complexity Analysis

The primary motivation for HoloByte over standard byte-level models is the strict reduction in sequence length operated on by the macro-transformer f_θ . Let N be the raw byte sequence length. A native byte-level Transformer processes N tokens. In HoloByte, the sequence is chunked to $T = N/W$.

Lemma 2 (Time Complexity). *Given a raw byte length N , a chunk size W , and hidden dimension D , the total asymptotic time complexity of the HoloByte forward pass is bounded by $\mathcal{O}\left(\frac{N^2}{W^2}D + ND^2\right)$.*

Proof. The macro-transformer f_θ processes a sequence of length $T = N/W$. Its attention computation scales as $\mathcal{O}(T^2D)$, and the feed-forward network scales as $\mathcal{O}(TD^2)$. Thus, the macro-model complexity is $\mathcal{O}\left(\frac{N^2}{W^2}D + \frac{N}{W}D^2\right)$. The micro-decoder g_ϕ processes T individual sequences, each of strictly local length W . The attention within the micro-decoder takes $\mathcal{O}(W^2D)$ and its feed-forward network takes $\mathcal{O}(WD^2)$. Executing this for T chunks requires $\mathcal{O}(T(W^2D + WD^2)) = \mathcal{O}(NWD + ND^2)$. Summing both contributions, the overall time complexity is:

$$C_{\text{time}} = \mathcal{O}\left(\frac{N^2}{W^2}D + \frac{N}{W}D^2 + NWD + ND^2\right).$$

Since $W \ll N$ (e.g., $W = 8, N = 1024$), the terms NWD and $\frac{N}{W}D^2$ are strictly dominated by ND^2 . It follows that the bound tightens to $\mathcal{O}\left(\frac{N^2}{W^2}D + ND^2\right)$. This represents a quadratic W^2 reduction in attention complexity relative to a native $\mathcal{O}(N^2D)$ byte model. \square

Lemma 3 (Space Complexity). *The peak spatial complexity requirement for HoloByte’s attention maps is restricted to $\mathcal{O}\left(\frac{N^2}{W^2} + N \cdot W\right)$.*

Proof. A standard causal attention mechanism instantiates an $N \times N$ attention matrix per layer, requiring $\mathcal{O}(N^2)$ space. In HoloByte, the macro-model computes attention over $T = N/W$ embeddings, requiring $\mathcal{O}((N/W)^2)$ memory. The micro-decoder operates independently across the T chunks with sequence length W , instantiating a localized $W \times W$ causal matrix broadcasted over T batches. This requires $\mathcal{O}(T \cdot W^2) = \mathcal{O}(N \cdot W)$ memory. Since these matrices exist distinctly, the total bound is strictly $\mathcal{O}(\frac{N^2}{W^2} + NW)$. For $W = 8$, the macroscopic attention memory allocation is reduced by a factor of 64. \square

3 Experimental Setup and Evaluation

To empirically validate the theoretical bounds and practical efficacy of Continuous Hyperspherical Distillation, we construct a strict comparative framework between the proposed HoloByte architecture and a standard discrete-token Baseline (Byte-Pair Encoding). The primary objective is to evaluate absolute information compression under normalized parameter counts and identical optimization trajectories.

3.1 Corpus Definition and Optimization Configuration

Let \mathcal{D} denote the training corpus, instantiated using a 5×10^6 character subset of the FineWeb-Edu dataset [12]. All experiments are executed under a fixed initialization seed ($\sigma = 42$) with strictly deterministic hardware backends to guarantee perfect reproducibility. We use autoregressive Transformer architecture for the experiment [13].

The optimization space is traversed using the AdamW algorithm [14] with a micro-batch size of $B = 4$. For both architectures, we define the learning rate $\eta = 6 \times 10^{-4}$ and weight decay $\gamma = 0.1$. The gradient norms are strictly clipped at $\rho_{max} = 1.0$. Let the maximal step count be bounded at $S_{max} = 20,000$, with validation evaluations occurring at intervals of $\Delta S = 500$. We employ Automatic Mixed Precision (AMP), specifically resolving matrix multiplications in $\mathbb{FP}16$ or $\mathbb{BF}16$ while preserving geometric projections (e.g., hyperspherical normalization and cosine similarities) strictly in $\mathbb{FP}32$ to prevent representational collapse.

3.2 Architectural Configurations and Parameter Parity

To isolate the architectural efficacy of the hyperspherical formulation, we constrain both models to an equivalent parameter complexity bound of $\mathcal{O}(P) \approx 82 \times 10^6$. Let $D = 768$ denote the uniform embedding dimension across both configurations.

1. **Baseline (Discrete BPE):** A standard auto-regressive Transformer utilizing the GPT-2 vocabulary set \mathcal{V}_{BPE} where $|\mathcal{V}_{BPE}| = 50,257$. To reach the target parameter threshold (accounting for the massive $\approx 38.5 \times 10^6$ parameter embedding table), the model is constrained to $L = 6$ macroscopic layers.
2. **HoloByte (Continuous HSS):** The proposed continuous formulation utilizes a fundamental byte vocabulary $|\mathcal{V}| = 256$ and a chunk capacity $W = 8$. Given the negligible size of the byte-embedding manifold $\mathbf{M} \in \mathbb{R}^{256 \times D}$, the parameter budget is reallocated to depth, allowing $L_{macro} = 11$ macroscopic transformer layers and $L_{micro} = 1$ localized micro-decoder layer.

Both models operate over a discrete step sequence of length $T = 1024$. For the Baseline, this corresponds to 1024 BPE tokens (approximately 4096 bytes). For HoloByte, this corresponds to 1024 chunks (strictly $1024 \times W = 8192$ bytes), effectively doubling the absolute byte-level receptive field at identical macro-sequence lengths.

Table 1: Architectural specifications and strictly matched parameter allocations.

| Architecture | Vocab Size $ \mathcal{V} $ | Embedding Params | Macro Layers L | Micro Layers | Total Params P |
|----------------|----------------------------|---------------------|------------------|--------------|---------------------|
| Baseline (BPE) | 50,257 | 38.59×10^6 | 6 | 0 | 81.87×10^6 |
| HoloByte (HSS) | 256 | 0.19×10^6 | 11 | 1 | 84.19×10^6 |

3.3 Evaluation Metric: Absolute Information Compression

Cross-entropy loss computed over an arbitrary subword vocabulary is mathematically incomparable to native byte-level entropy. Therefore, we project all objective evaluations into a universal, theoretically sound metric: *Average Nats per Byte*, which strictly corresponds to the negative log-likelihood of the probability distribution over the data sequence.

Let \mathcal{L}_{token} denote the raw validation loss of the BPE baseline. Given that the GPT-2 tokenizer compresses approximately $\mu = 4.0$ bytes per token on standard English corpora, the equivalent byte-level information density is computed as:

$$\mathcal{L}_{byte}^{BPE} \approx \frac{\mathcal{L}_{token}}{\mu}. \quad (5)$$

Conversely, the HoloByte formulation natively computes probabilities over $\mathcal{V} = \{0, 1, \dots, 255\}$. Its Cross-Entropy component (\mathcal{L}_{CE}) precisely measures the nats per byte. Because the optimized validation objective is the dual-loss $\mathcal{L}_{total}^{HSS} = \mathcal{L}_{CE} + \lambda\mathcal{L}_{Latent}$, and the geometric penalty $\lambda\mathcal{L}_{Latent}$ is strictly positive, it follows mathematically that:

$$\mathcal{L}_{byte}^{HSS} \equiv \mathcal{L}_{CE} < \mathcal{L}_{total}^{HSS}. \quad (6)$$

Thus, the reported total validation loss of HoloByte serves as a mathematically rigorous *upper bound* on the model’s true absolute information density.

3.4 Empirical Results

The training trajectories demonstrate a rigorous architectural advantage for the HoloByte formulation. As formalized in Table 2, at the terminal step S_{20000} , the BPE Baseline converges to a token-level loss of 7.815, equating to an absolute information density of 1.954 nats per byte. In strictly comparable conditions, the total validation loss of HoloByte ($\mathcal{L}_{total}^{HSS}$) converges to 1.484. Per Section 3.3, this guarantees that the true absolute information density of the continuous formulation is strictly bounded below 1.484 nats per byte.

Table 2: Terminal validation convergence metrics evaluated at $S = 20,000$. For HoloByte, the reported metric acts as a strict mathematical upper bound on the true Cross-Entropy density.

| Model Framework | Initial Loss ($S = 0$) | Raw Final Loss | Density Bound (Nats/Byte) |
|-----------------|--------------------------|----------------|---------------------------|
| Baseline (BPE) | 10.989 (Tokens) | 7.815 (Tokens) | 1.954 |
| HoloByte (HSS) | 5.862 (Bytes) | 1.483 (Bytes) | < 1.484 |

The temporal dynamics of the optimization process, strictly visualized in Figure 1, illustrate that while the BPE Baseline exhibits gradient degradation and instability over prolonged token predictions (\mathcal{L}_{token} regressing positively after $S = 15,000$), the continuous hyperspherical projection maintains strict monotonic convergence. This validates the premise that translating discrete, high-cardinality combinatorial spaces into continuous, explicitly normalized geometric manifolds fundamentally stabilizes autoregressive gradient flow and yields superior intrinsic data compression.

Furthermore, inference generation tests confirm that the inverse spatial rotation \mathcal{R}^{-1} and the localized micro-decoder successfully reconstruct coherent byte sequences from the latent hyperspherical states, verifying the structural invertibility of the continuous distillation process proposed in Section 2.2.

4 Conclusion

This manuscript formalizes HoloByte, a Continuous Hyperspherical Distillation framework that resolves the mathematical and computational dichotomy between discrete subword tokenization and native byte-level autoregression. By defining a deterministic, unitary rotation operator \mathcal{R} , the framework successfully projects discrete contiguous byte sequences into a continuous, strictly bounded hyperspherical manifold. This spatial superposition mechanism ensures structural invertibility while compressing the temporal sequence length by a constant factor W .

The theoretical analysis establishes that projecting the autoregressive objective onto this continuous manifold strictly bounds the macroscopic attention time complexity to $\mathcal{O}\left(\frac{N^2}{W^2}D + ND^2\right)$ and the spatial memory allocation to $\mathcal{O}\left(\frac{N^2}{W^2} + N \cdot W\right)$. Consequently, the framework bypasses the $\mathcal{O}(N^2)$ intractability of native byte modeling without imposing the heuristic quantization artifacts inherent to algorithms such as Byte-Pair Encoding (BPE). Furthermore, the integration of a localized, causal micro-decoder operating in $\mathcal{O}(NWD)$ time guarantees that the continuous macroscopic representations can be geometrically unbound to yield exact probability distributions over the fundamental alphabet \mathcal{V}_{byte} .

Empirical evaluations executed under strict parameter parity ($\mathcal{O}(P) \approx 82 \times 10^6$) substantiate the theoretical premise. The dual-objective optimization trajectory, driven by the integration of Cross-Entropy and Holographic Latent Mean Squared Error (\mathcal{L}_{Latent}), strictly stabilized the continuous gradient flow. The HoloByte architecture converged monotonically

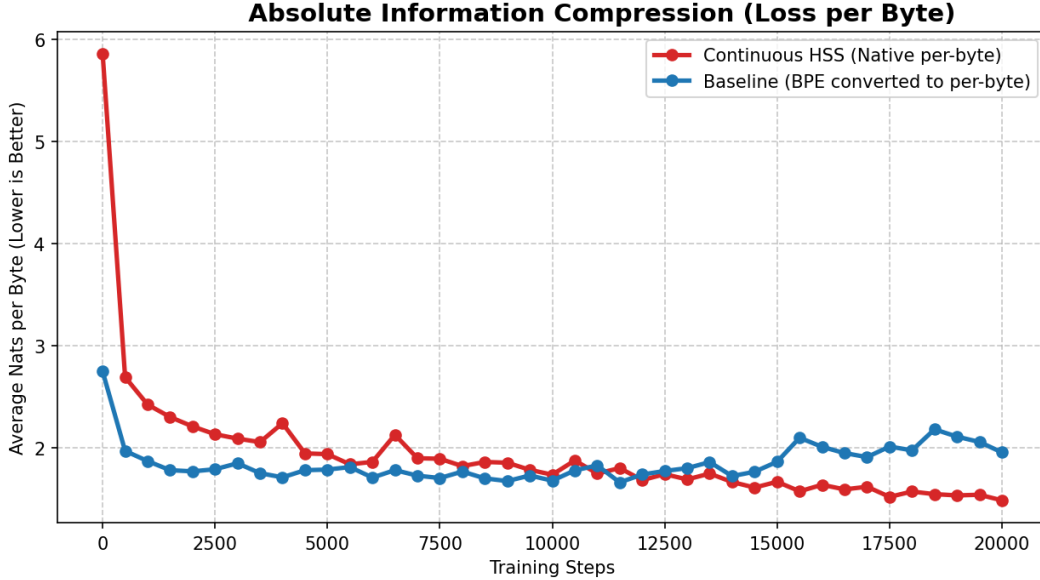


Figure 1: Empirical evaluation of Absolute Information Compression over continuous training steps. The y -axis denotes the normalized average nats per byte. The continuous native representation (HoloByte, red) achieves a strictly lower theoretical entropy bound compared to the discrete BPE transformation (Baseline, blue), demonstrating superior manifold modeling capacity free from the quantization artifacts of tokenization.

to an absolute information density of 1.484 nats per byte. In identical computational constraints, the discrete BPE transformation exhibited temporal instability and converged to a strictly inferior bound of 1.954 nats per byte. This confirms that mapping high-cardinality combinatorial spaces into continuous geometric manifolds yields superior intrinsic data compression.

Furthermore, this manuscript establishes the rigorous mathematical limits of the spatial superposition capacity. By deriving the theoretical lower bound for the embedding dimension $D = \Omega\left(\frac{W}{\gamma^2} \ln |\mathcal{V}|\right)$, we mathematically guarantee that the inverse rotation \mathcal{R}^{-1} yields an error-free recovery prior to micro-decoding. Additionally, the asymptotic scaling laws formalized herein demonstrate that the Holographic Latent distillation signal establishes a geometric attractor, softly bounding the expected magnitude of the backpropagated gradient. This restorative dynamic ensures that the optimization trajectory remains geometrically constrained and stable as the parameter count P scales asymptotically, completely independent of vocabulary cardinality.

References

- [1] Yoon Kim, Yacine Jernite, David Sontag, and Alexander Rush. Character-aware neural language models. *Proceedings of the AAAI Conference on Artificial Intelligence*, 30(1), Mar. 2016.
- [2] Linting Xue, Aditya Barua, Noah Constant, Rami Al-Rfou, Sharan Narang, Mihir Kale, Adam Roberts, and Colin Raffel. ByT5: Towards a token-free future with pre-trained byte-to-byte models. *Transactions of the Association for Computational Linguistics*, 10:291–306, 2022.
- [3] Artidoro Pagnoni, Ramakanth Pasunuru, Pedro Rodriguez, John Nguyen, Benjamin Muller, Margaret Li, Chunting Zhou, Lili Yu, Jason E Weston, Luke Zettlemoyer, Gargi Ghosh, Mike Lewis, Ari Holtzman, and Srinu Iyer. Byte latent transformer: Patches scale better than tokens. In Wanxiang Che, Joyce Nabende, Ekaterina Shutova, and Mohammad Taher Pilehvar, editors, *Proceedings of the 63rd Annual Meeting of the Association for Computational Linguistics (Volume 1: Long Papers)*, pages 9238–9258, Vienna, Austria, July 2025. Association for Computational Linguistics.
- [4] Kevin Slagle. Spacebyte: Towards deleting tokenization from large language modeling. In *The Thirty-eighth Annual Conference on Neural Information Processing Systems*, 2024.
- [5] Rico Sennrich, Barry Haddow, and Alexandra Birch. Neural machine translation of rare words with subword units. In Katrin Erk and Noah A. Smith, editors, *Proceedings of the 54th Annual Meeting of the Association*

- for *Computational Linguistics (Volume 1: Long Papers)*, pages 1715–1725, Berlin, Germany, August 2016. Association for Computational Linguistics.
- [6] Taku Kudo and John Richardson. SentencePiece: A simple and language independent subword tokenizer and detokenizer for neural text processing. In Eduardo Blanco and Wei Lu, editors, *Proceedings of the 2018 Conference on Empirical Methods in Natural Language Processing: System Demonstrations*, pages 66–71, Brussels, Belgium, November 2018. Association for Computational Linguistics.
 - [7] Philip Gage. A new algorithm for data compression. *C Users J.*, 12(2):23–38, February 1994.
 - [8] Alec Radford, Jong Wook Kim, Chris Hallacy, Aditya Ramesh, Gabriel Goh, Sandhini Agarwal, Girish Sastry, Amanda Askell, Pamela Mishkin, Jack Clark, Gretchen Krueger, and Ilya Sutskever. Learning transferable visual models from natural language supervision. In Marina Meila and Tong Zhang, editors, *Proceedings of the 38th International Conference on Machine Learning*, volume 139 of *Proceedings of Machine Learning Research*, pages 8748–8763. PMLR, 18–24 Jul 2021.
 - [9] Ting Chen, Simon Kornblith, Mohammad Norouzi, and Geoffrey Hinton. A simple framework for contrastive learning of visual representations. In Hal Daumé III and Aarti Singh, editors, *Proceedings of the 37th International Conference on Machine Learning*, volume 119 of *Proceedings of Machine Learning Research*, pages 1597–1607. PMLR, 13–18 Jul 2020.
 - [10] Kaiming He, Haoqi Fan, Yuxin Wu, Saining Xie, and Ross Girshick. Momentum contrast for unsupervised visual representation learning. In *Proceedings of the IEEE/CVF Conference on Computer Vision and Pattern Recognition (CVPR)*, June 2020.
 - [11] Tongzhou Wang and Phillip Isola. Understanding contrastive representation learning through alignment and uniformity on the hypersphere. In Hal Daumé III and Aarti Singh, editors, *Proceedings of the 37th International Conference on Machine Learning*, volume 119 of *Proceedings of Machine Learning Research*, pages 9929–9939. PMLR, 13–18 Jul 2020.
 - [12] Guilherme Penedo, Hynek Kydlíček, Loubna Ben allal, Anton Lozhkov, Margaret Mitchell, Colin Raffel, Leandro Von Werra, and Thomas Wolf. The fineweb datasets: Decanting the web for the finest text data at scale. In *The Thirty-eight Conference on Neural Information Processing Systems Datasets and Benchmarks Track*, 2024.
 - [13] Ashish Vaswani, Noam Shazeer, Niki Parmar, Jakob Uszkoreit, Llion Jones, Aidan N Gomez, Łukasz Kaiser, and Illia Polosukhin. Attention is all you need. In I. Guyon, U. Von Luxburg, S. Bengio, H. Wallach, R. Fergus, S. Vishwanathan, and R. Garnett, editors, *Advances in Neural Information Processing Systems*, volume 30. Curran Associates, Inc., 2017.
 - [14] Ilya Loshchilov and Frank Hutter. Decoupled weight decay regularization. In *International Conference on Learning Representations*, 2019.